

HETG/LETG — Status

Chandra Quarterly Review No. 56

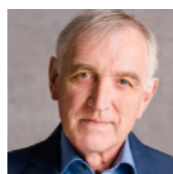
15 November 2023

David Huenemoerder
dph@space.mit.edu

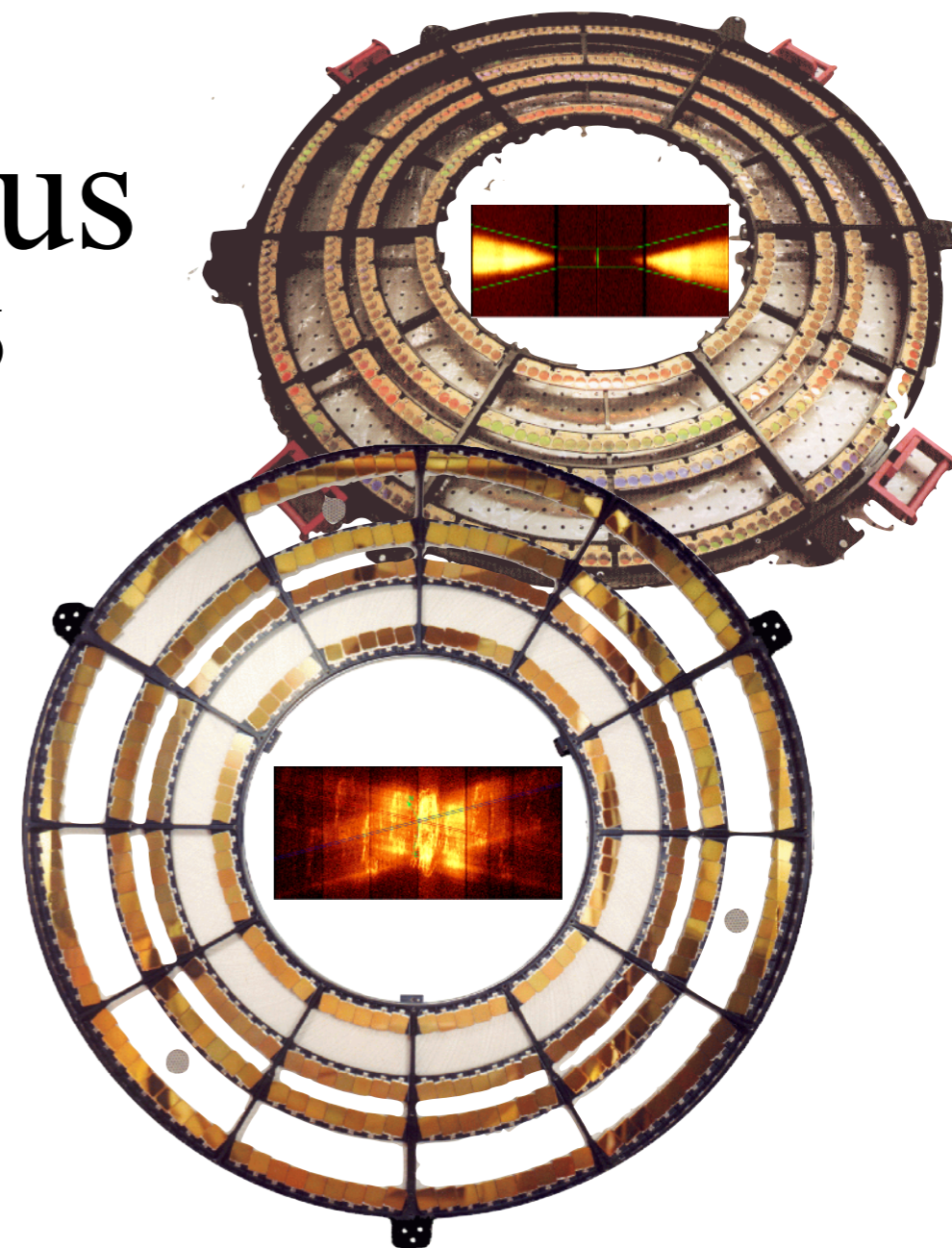
HETG IPI: Prof. Claude R. Canizares
MIT Kavli Institute



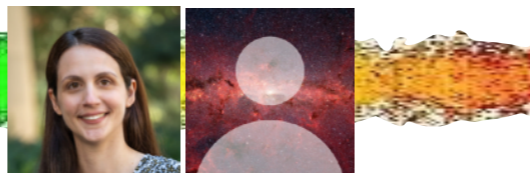
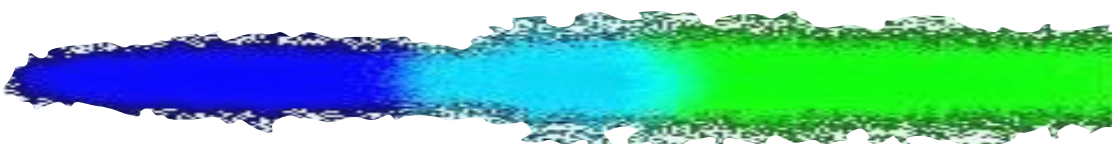
LETG IPIs: Dr. Peter Predehl
Max Planck Institute



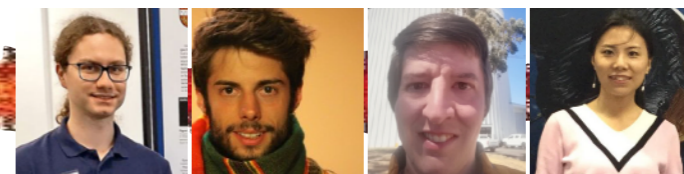
Dr. Jelle Kaastra
SRON



faculty, staff;



... current/incoming ...



... moved on ...



Proposal Cycle 23 Jan 2022 (637 ks)

- ★ Stars: π Aqr 101 ks Winds of the hottest stars
- ★ AGN: Circinus Galaxy 69 ks Emission lines, morphology, variability (IXPE-coordinated)
- ★ XRB: Cen X-3 61 ks Eclipsing X-ray pulsar; accretion
- ★ XRB: 4U 1626-67 86 ks Ultra-compact binary; monitor Fe lines.
- ★ XRB: GX 1+4 92 ks Low-mass XRB; accretion, Compton shoulder study.
- ★ ISM: GX 340+0 138 ks Cosmic dust composition
- ★ ULX/NS: M33 X-8 90 ks Pulsar wind outflow, absorption

Proposal Cycle 24 Jan 2023 (77 / 745 ks)

- ★ XRB: 4U 1624-490 29/135 ks Accretion disk structure (with NuSTAR, XRISM)
- ★ XRB: Cen X-3 48 ks Eclipsing X-ray pulsar; accretion (ongoing - low visibility)
- ★ AGN: MCG-6-30-15 0/232 ks Time-dependent photoionisation modeling of outflows
- ★ BH: SS 433 0/60 ks Relativistic jet physics (coordinated with HRC, Swift GO)
- ★ ULX: LMC/SMC X-? 0/70 ks Accretion disk outbursts (TOO)
- ★ NS: Terzan 5 X-2 0/200 ks Neutron Star outburst (TOO)

Jargon list:
 AGN: Active Galactic Nucleus
 BH: Black Hole
 ISM: InterStellar Medium
 NS: Neutron Star
 SN: SuperNova
 ULX: Ultra-Luminous X-ray source
 SNR: SuperNova Remnant
 XRB: X-ray Binary
 LMXB: Low Mass XRB

Proposal **Cycle 25** start Jan 2024 (758 ks; or 1208 ks if TOOs trigger)

- ★ XRB: 4U 1626-67 0/190 ks Accretion disk structure (with NuSTAR, XRISM)
- ★ Star ζ Puppis 0/190 ks Stellar Winds, long-term monitoring
- ★ XRB GRS 1915+105 0/100 ks micro-Quasar (TOO; coordinated with NICER, NuSTAR)
- ★ ISM GX 9+9 0/180 ks Galactic silicon absorption survey
- ★ ULX M33 X-8 0/85 ks Pulsar wind outflow, absorption
- ★ XRB Her X-1 0/50 ks Neutron star accretion disks (TOO)
- ★ NS: Terzan 5 X-2 0/200 ks Neutron Star outburst (TOO)
- ★ BH: GW Transient 0/300 ks Gravitational wave event followup (TOO)

Jargon list:

AGN: Active Galactic Nucleus

BH: Black Hole

ISM: InterStellar Medium

NS: Neutron Star

SN: SuperNova

ULX: Ultra-Luminous X-ray source

SNR: SuperNova Remnant

XRB: X-ray Binary

LMXB: Low Mass XRB



Proposal Cycle 23: (328 ks)

★ Stars (Predehl/MPE)	LTT 1445A	45 ks	High energy environments of terrestrial exoplanets (ACIS-S)
★ Stars (Predehl/MPE)	L 168-9	24 ks	High energy environments of terrestrial exoplanets (ACIS-S)
★ SNR (Predehl/MPE)	Hoinga	59 ks	Distance determination (HRC-I, ACIS-I)
★ AGN (Predehl/MPE)	WISEA J202040.85-621509.3	30 ks	Confirm eRosita detection of a z=5.9 quasar (ACIS-S)
★ Galaxies (Kaastra/SRON)	Abell 141	170 ks	Intercluster temperatures, merger history (ACIS-S)

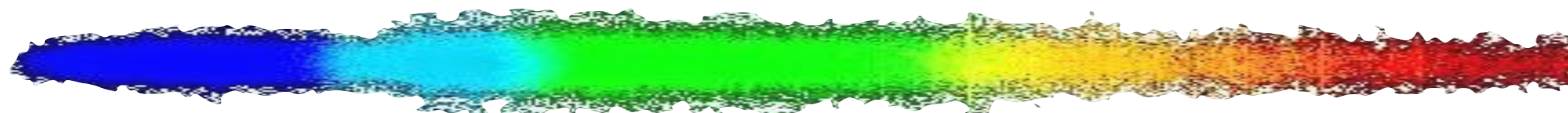
Proposal Cycle 24: start Jan 2023 (0 / 337 ks)

★ AGN: (Predehl/MPE)	WISEA J050222.16-341201.6	0/25 ks	Luminous z>5.6 quasars from eROSITA (ACIS-S)
★ AGN: (Predehl/MPE)	WISEA J230341.02-542730.6	0/32	Luminous z>5.6 quasars from eROSITA (ACIS-S)
★ AGN: (Predehl/MPE)	WISEA J050411.92-254959.0	0/26	Luminous z>5.6 quasars from eROSITA (ACIS-S)
★ Galaxies: (Predehl/MPE)	eFEDSJ083933	0/88	Shocks in an eROSITA detected galaxy cluster (ACIS-S)
★ AGN: (Kaastra/SRON)	NGC 3783	0/166	Outflows, variability (with XRISM) (ACIS-S)

Proposal Cycle 25 start Jan 2024 (343 ks)

★ ISM: (Predehl/MPE)	HD 115247	0/59 ks	Galactic bubbles absorption (w/ eROSITA)
★ ISM: (Predehl/MPE)	HE1338-1423	0/59 ks	Galactic bubbles absorption (w/ eROSITA)
★ ISM: (Predehl/MPE)	LEDA407	0/59 ks	Galactic bubbles absorption (w/ eROSITA)
★ AGN: (Kaastra/SRON)	A1550	0/166 ks	Outflows, variability

AGN: Active Galactic Nucleus
 BH: Black Hole
 ISM: InterStellar Medium
 NS: Neutron Star
 SN: SuperNova
 ULX: Ultra-Luminous X-ray source
 SNR: SuperNova Remnant
 XRB: X-ray Binary
 LMXB: Low Mass XRB



Performance May 2023 — Oct 2023

HETG/ACIS-S: 842 ks

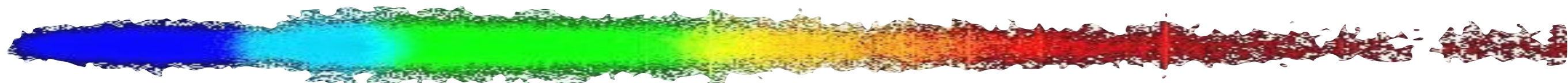
- 44 observations on 13 targets (26 GO, 9 GTO, 6 TOO, 3 DDT, 0 Cal)

LETG: 603 ks

- 32 LETG/HRC-S observations, 5 targets (368 ks; 14 GO, 11 GTO, 5 TOO)
- 15 LETG/ACIS-S observations, 2 targets (233 ks; 15 Cal — contamination)
- 1 LETG/HRC-I observation, 1 target (2 ks; Cal — low E response)

All instruments: 11,383 ks

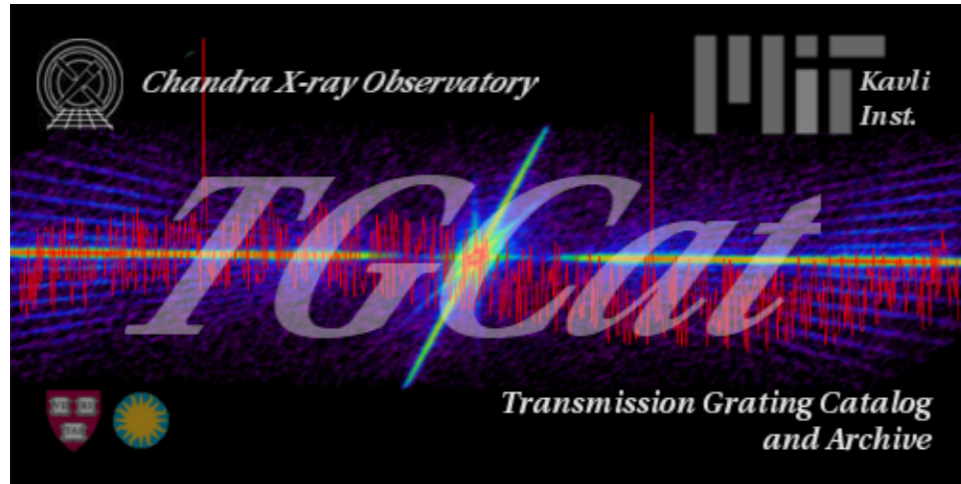
Grating performance is nominal.





MIT KAVLI INSTITUTE

TGCat Status



... has been *off-line Sept–Oct 2023* for maintenance/ system upgrades. It has existed since 2008 – if unfamiliar with it, see Chandra Newsletter #16 (Winter 2009, <https://cxc.harvard.edu/newsletters/news_16/news16_p33.html>) or Huenemoerder et al 2011 (<<https://ui.adsabs.harvard.edu/abs/2011AJ....141..129H/abstract>>)

Back on-line as of ...

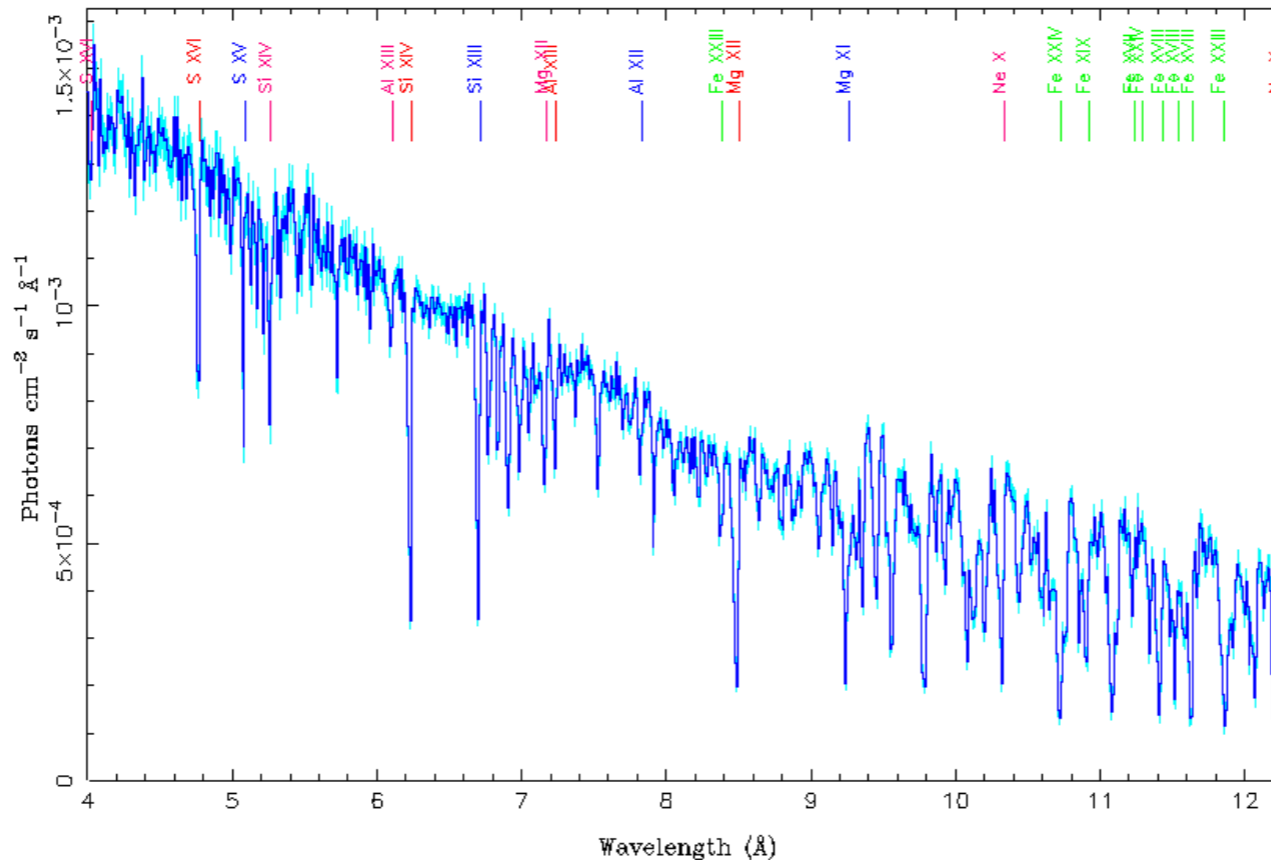
<http://tgcate.mit.edu>

Multi Preview

combined extraction product

object	Multi Preview
obsid	373, 2090, 2091, 2092, ... target='blank'> 373, 2090, 2091, 2092, ...
ids	3553, 3695, 3696, 3698, ...
srcids	1666
instruments	ACIS
gratings	HETG
total_exposure(s)	1.20e+6
ra	174.75710
decl	-37.73863
heg_band(c/s)	7.86e-1
meg_band(c/s)	8.07e-1
leg_band(c/s)	7.95e-1
letg_acis_band(c/s)	7.95e-1
zeroth_order(c/s)	2.52e-1
proc_date	2013-08-18 17:38:08.1000
date_obs	2006-08-09 06:08:45.5000

PLOTTING CONTROLS



Example interactive plot: NGC 3783, 10 observations with HETG, 1.2 Ms, all-combined flux plot.

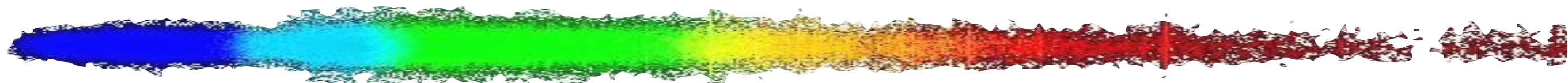
<<http://tgcat.mit.edu/dev/tgcat/tgTrend.php>>



ACIS High-T Operations: OK to use HETG
(but for warmest temperatures, offset to low CHIPY).

HETG 2nd and 3rd order efficiencies: in progress.

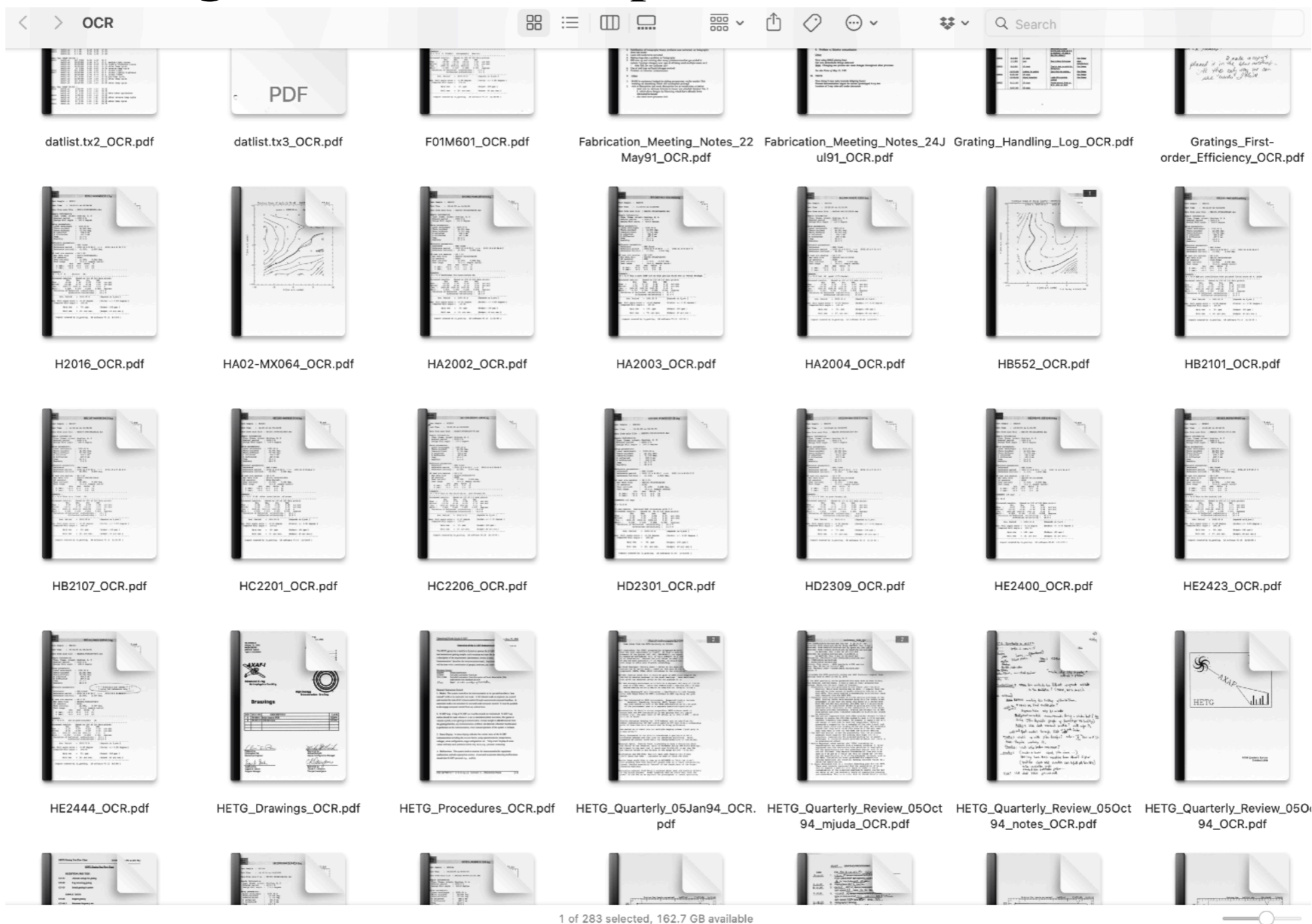
Line-spread-function parameters for HETG/HRC-I and off-axis pointings: in progress.



Before scanning ... about 30 binders:



... after scanning: 283 searchable pdf files:



OCR

Search

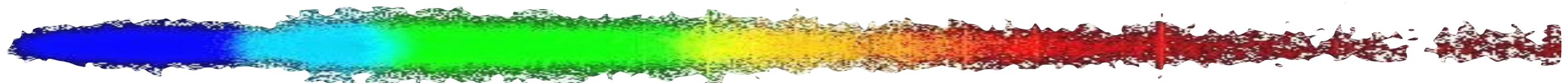
datelist.tx2_OCR.pdf datelist.tx3_OCR.pdf F01M601_OCR.pdf Fabrication_Meeting_Notes_22_May91_OCR.pdf Fabrication_Meeting_Notes_24J_ul91_OCR.pdf Grating_Handling_Log_OCR.pdf Gratings_First-order_Efficiency_OCR.pdf

H2016_OCR.pdf HA02-MX064_OCR.pdf HA2002_OCR.pdf HA2003_OCR.pdf HA2004_OCR.pdf HB552_OCR.pdf HB2101_OCR.pdf

HB2107_OCR.pdf HC2201_OCR.pdf HC2206_OCR.pdf HD2301_OCR.pdf HD2309_OCR.pdf HE2400_OCR.pdf HE2423_OCR.pdf

HE2444_OCR.pdf HETG_Drawings_OCR.pdf HETG_Procedures_OCR.pdf HETG_Quarterly_05Jan94_OCR.pdf HETG_Quarterly_Review_05Oct_94_mjuda_OCR.pdf HETG_Quarterly_Review_05Oct_94_notes_OCR.pdf HETG_Quarterly_Review_05Oct_94_OCR.pdf

1 of 283 selected, 162.7 GB available

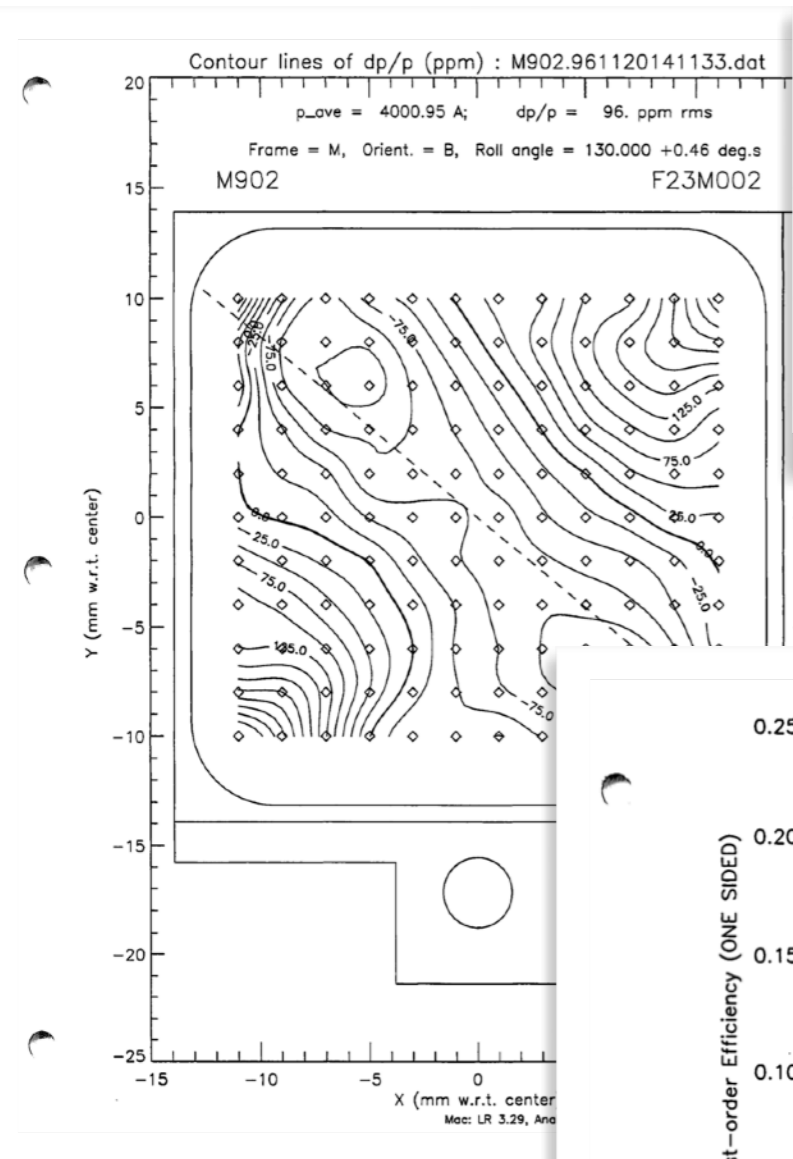




MIT KAVLI INSTITUTE

Technical details of grating facet fabrication, measurement, modeling, instrument assembly, test, requirements documents, meeting notes, ...

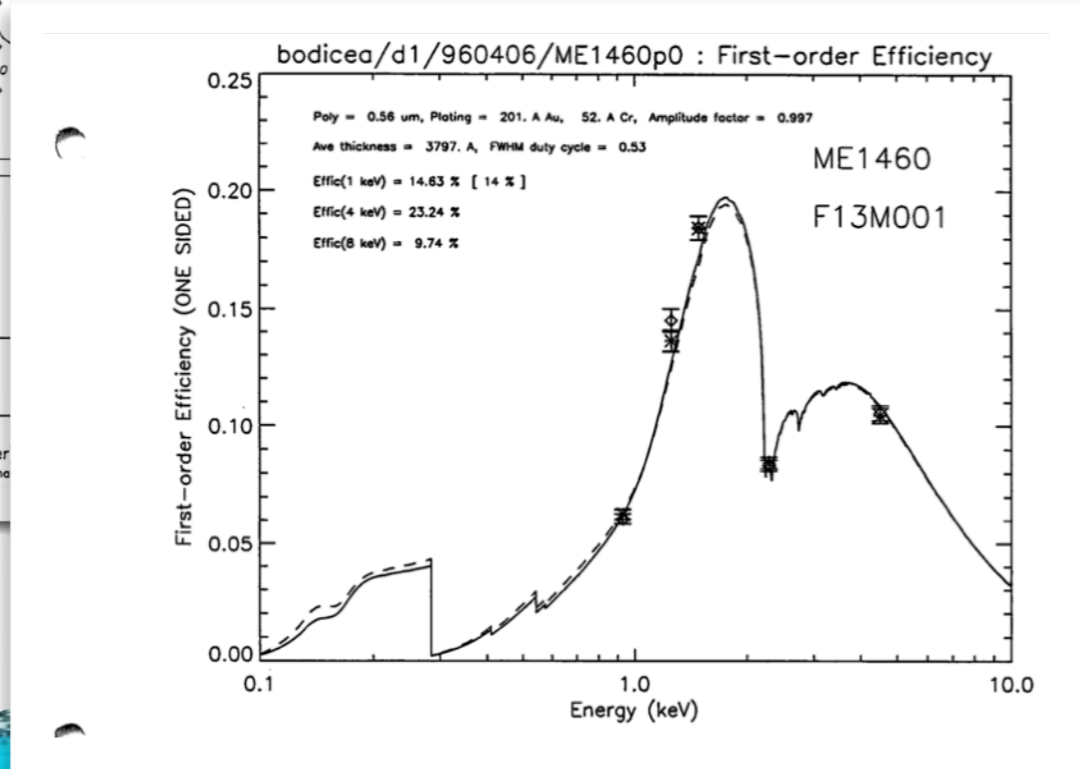
Items of historical interest...



UV Test of Grating HX044 Date 7/21/90
 Fabrication number JP 5-15-90-41
 Data file hx044n1.dat
 Temp./ Humidity 27.5°C / 74% / 11.26 gm $X_w = 4.50$
 Other Conditions: *Some mask clamps tightened only until 'catching' of grating.* Cal = 7/26/90

Grating		Measurement		Spots	Comments
x _g	y _g	x _m	y _m		
5.5	3.00	13.87	10.84	6	blurred

Handwritten notes: 0.60, 14.20, 5.30, 23.65, 20.70, 2.15, 11:30pm



AGENDA

AXAF Quarterly Review
 MSFC
 10/29/93
HETG

- Program Schedule
- Process Development
- Facility Status
- Mechanical Design
- Systems/Programs Issues
- Key Milestones



THE ASTROPHYSICAL JOURNAL, 956:65 (13pp), 2023 October 10

© 2023. The Author(s). Published by the American Astronomical Society.

OPEN ACCESS

<https://doi.org/10.3847/1538-4357/acd49>



Systematic Uncertainties of Atomic Data in Photoionization Modeling

R. Ballhausen^{1,2}, T. R. Kallman², L. Gu^{3,4,5}, and F. Paerels⁶

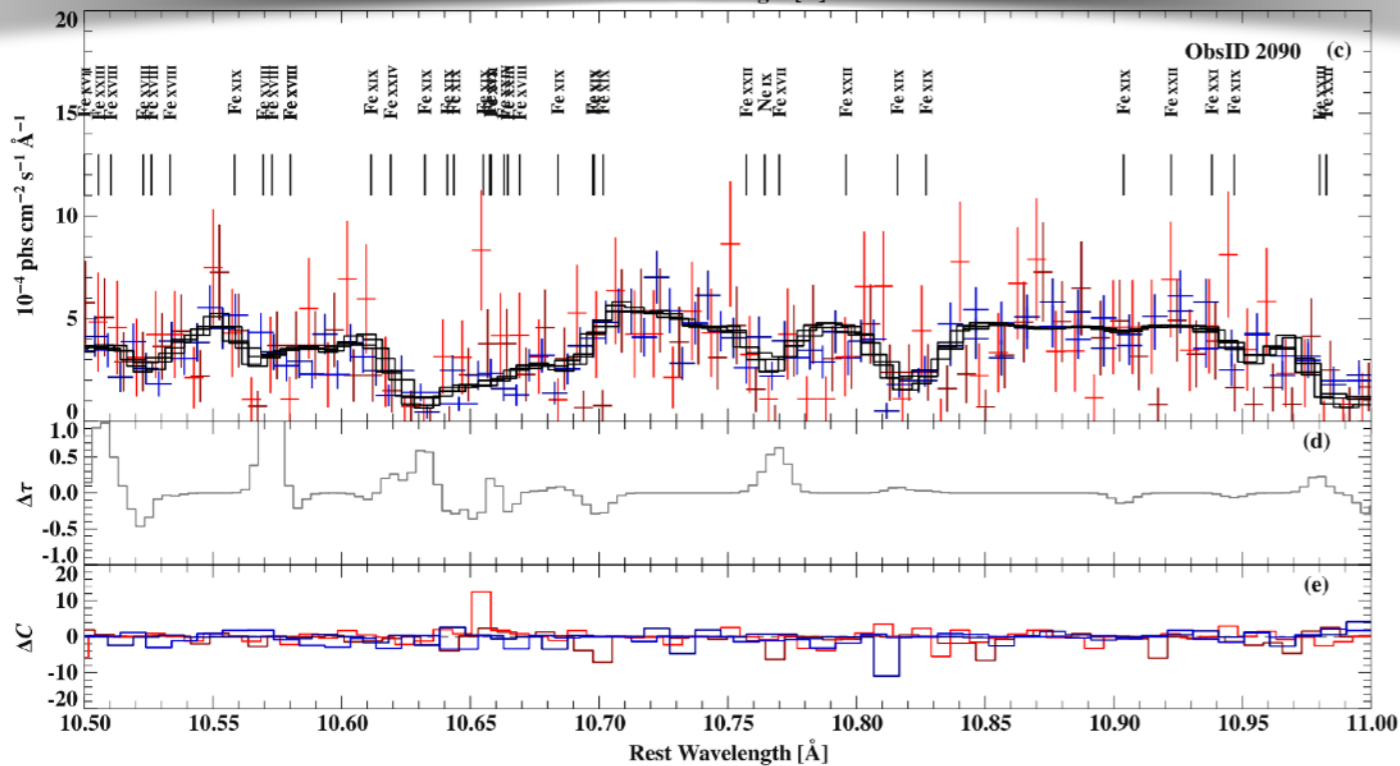
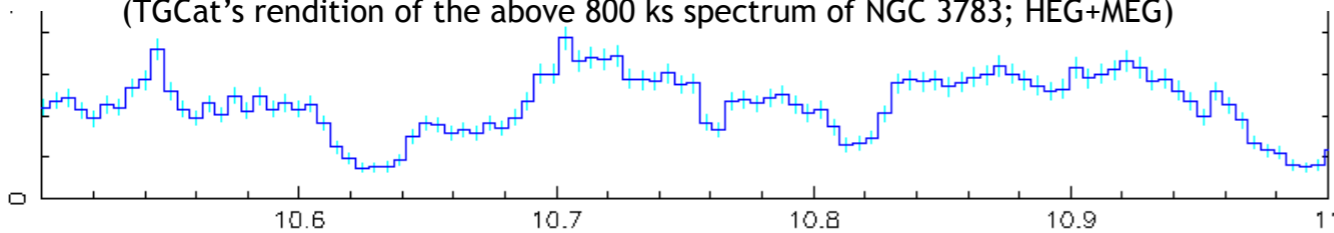


Figure 3. (a) Close-up of the HEG (red) and MEG (blue) 10.5–11.0 Å spectra of the NGC 3783 observation 2090 fitted with a five-component warmabs model (black). (b) C-residuals for the baseline model. (c) Same data as in (a) but with the warmabs model modified by the additional Gaussian lines. (d) Additional optical depth $\Delta\tau$ that is added or removed from each bin by the Gaussian components. (e) C-residuals for the modified model. As shown here and described in Section 5.1, including additional Gaussians—equivalent to modifying A-values for the strongest 500 lines—leads only to minor to moderate improvement of the fit statistics and residuals.

(TGCat's rendition of the above 800 ks spectrum of NGC 3783; HEG+MEG)



Abstract

Fitting plasma models to high-quality spectra is a crucial tool for deriving diagnostics about the physical conditions in various astrophysical sources. Despite decades of model development, this prescription often provides an unsatisfying description of observational data. We explore some of the origins of the failure of fits of photoionized plasma models to high-resolution X-ray spectra. In particular, we test whether systematic uncertainties in underlying atomic data can account for data model discrepancies, and whether including model uncertainties during spectral fitting can provide statistically acceptable fits and reasonable parameter estimates. We fit Chandra/HETG spectra of NGC 3783 with the photoionized absorber model warmabs. We use the remaining data model residuals to estimate the systematic uncertainties of bound-bound radiative rates for individual transitions. We then include these uncertainties into warmabs to return a total model uncertainty. We find that residual data model discrepancies which are due to systematic errors that cannot be accounted for solely by the modification of the optical depth of strong absorption lines. Furthermore, statistical uncertainties still dominate the fit residuals on a case-by-case basis. However, we conclude that while the current uncertainties in radiative rates cannot be held solely responsible for statistically unacceptable fits, other sources of uncertainty in the atomic data investigation.

... we test whether systematic uncertainties in underlying atomic data can account for data model discrepancies, and whether including model uncertainties during spectral fitting can provide statistically acceptable fits and reasonable parameter estimates. We fit Chandra/HETG spectra of NGC 3783 with the photoionized absorber model warmabs.

6. Conclusions and Outlook

We reanalyzed a set of archival Chandra/HETG observations of NGC 3783 and modeled the warm absorber in this source with the xstar-derived absorption model warmabs in order to characterize the quality of the photoionization model and the underlying atomic data, and to understand the remaining data model residuals that often lead to statistically unacceptable fits.

We conclude that inaccuracies of radiative transition rates are not a major source of data model discrepancies. Our fits to simulated spectra further show that in the majority of practical cases of currently available observational data, statistical uncertainties dominate the accuracy to which plasma parameters can be constrained.



Some Scientific Results Published in the Past 6 Months (2/2)



Monthly Notices
of the
ROYAL ASTRONOMICAL SOCIETY
MNRAS 522, L66–L71 (2023)
Advance Access publication 2023 March 25
https://doi.org/10.1093/mnras/522/L66

A detailed analysis of X-ray emission-line velocities of Capella from over 20 yr of *Chandra*/HETG spectroscopy

E. Bozzo^{1*}, D. P. Huenemoerder², N. Produit¹, M. Falanga^{3,4}, S. Paltani¹ and E. Costantini^{5,6}

Capella doppler velocity measurements L69

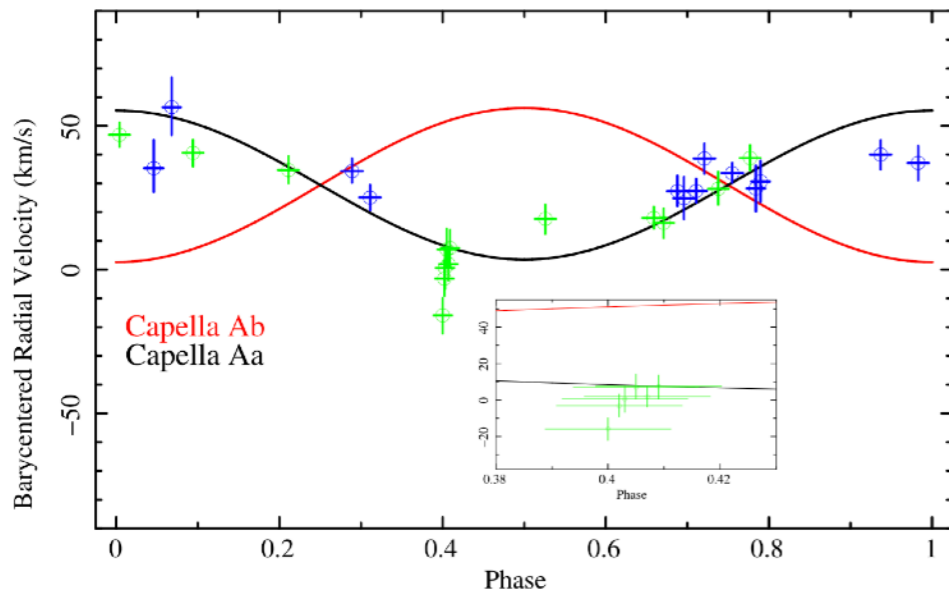


Figure 1. Plot of the barycentred radial velocity measurements (green and blue points) obtained from all available *Chandra*/HETG observations of Capella (see Table 1). The blue points correspond to observations that were not reported before by ISH06. The error bars for each radial velocity measurement are given at 1σ c.l. and are only statistical. The uncertainty on the phase for each green point includes the duration of the observation, as well as the uncertainties associated with the ephemerides. The black and red lines are the expected barycentred radial velocities calculated according to the latest Capella's orbital parameters published by Strassmeier et al. (2020). Uncertainties on these velocities were not included here as they are typically $\ll 1 \text{ km s}^{-1}$. The phase 0 is assumed as the epoch of passage at the ascending node. The insert shows, for clarity, a zoom around the orbital phase 0.4 showing six observations closely overlapping in phase.

3 RESULTS AND DISCUSSION

All results of our analysis are summarized in Fig. 1. The black and red lines represent the barycentred radial velocity along the orbits of the two Capella components (Aa and Ab) derived from the orbital parameters as in Strassmeier et al. (2020). The green points with the error bars represent the barycentred Doppler

“The 13 new observations reported here for the first time strengthen some of the previous conclusions...

... more firmly establishes that Capella Aa is the dominant X-ray emitter

... an overall uncertainty for the averaged barycentered radial velocity that is of other order of $\sim 20 \text{ km s}^{-1}$ (at 3σ c.l.).

... the stability of the instrument (and the accuracy of the performed in-flight calibrations) achieving now a baseline of over 22 yr.”

MNRAS 000, 1–?? (0000)

Preprint 2 November 2023

Compiled using MNRAS L^AT_EX style file v3.0

(submitted)

Chandra/HETG Doppler velocity measurements in stellar coronal sources

E. Bozzo^{1*}, D. P. Huenemoerder², M. Falanga^{3,4}, S. Paltani¹, E. Costantini^{5,6}, J. de Plaa⁵

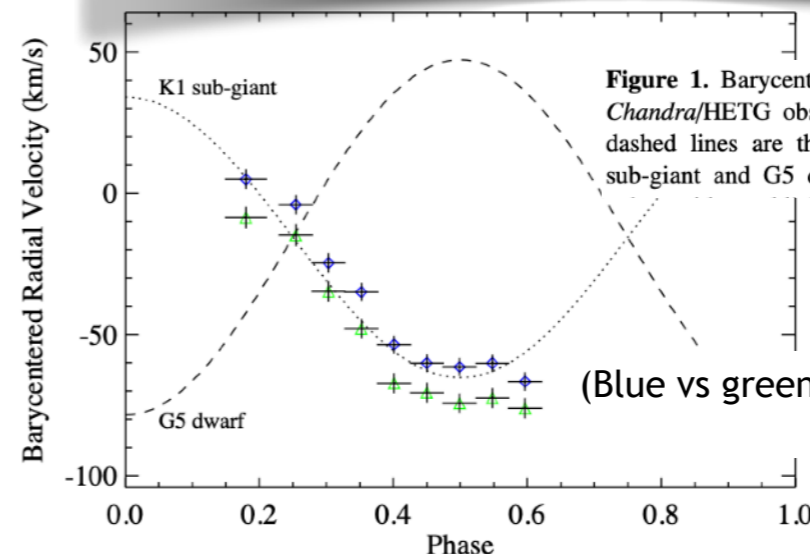


Figure 1. Barycentred radial velocity measurements obtained from the *Chandra*/HETG observations of HR 1099 (see Table 1). The dotted and dashed lines are the expected barycentred radial velocities of the K1 sub-giant and G5 dwarf stars

(Blue vs green: atomic database systematics)

